



TECH BRIEFS

NATIONAL AERONAUTICS AND SPACE ADMINISTRATION

-  **Technology Focus**
-  **Electronics/Computers**
-  **Software**
-  **Materials**
-  **Mechanics/Machinery**
-  **Manufacturing**
-  **Bio-Medical**
-  **Physical Sciences**
-  **Information Sciences**
-  **Books and Reports**

INTRODUCTION

Tech Briefs are short announcements of innovations originating from research and development activities of the National Aeronautics and Space Administration. They emphasize information considered likely to be transferable across industrial, regional, or disciplinary lines and are issued to encourage commercial application.

Additional Information on NASA Tech Briefs and TSPs

Additional information announced herein may be obtained from the NASA Technical Reports Server: <http://ntrs.nasa.gov>.

Please reference the control numbers appearing at the end of each Tech Brief. Information on NASA's Innovative Partnerships Program (IPP), its documents, and services is available on the World Wide Web at <http://www.ipp.nasa.gov>.

Innovative Partnerships Offices are located at NASA field centers to provide technology-transfer access to industrial users. Inquiries can be made by contacting NASA field centers listed below.

NASA Field Centers and Program Offices

Ames Research Center

Mary Walsh
(650) 604-1405
mary.w.walsh@nasa.gov

Dryden Flight Research Center

Ron Young
(661) 276-3741
ronald.m.young@nasa.gov

Glenn Research Center

Joe Shaw
(216) 977-7135
robert.j.shaw@nasa.gov

Goddard Space Flight Center

Nona Cheeks
(301) 286-5810
nona.k.cheeks@nasa.gov

Jet Propulsion Laboratory

Indrani Graczyk
(818) 354-2241
indrani.graczyk@jpl.nasa.gov

Johnson Space Center

John E. James
(281) 483-3809
john.e.james@nasa.gov

Kennedy Space Center

David R. Makufka
(321) 867-6227
david.r.makufka@nasa.gov

Langley Research Center

Michelle Ferebee
(757) 864-5617
michelle.t.ferebee@nasa.gov

Marshall Space Flight Center

Jim Dowdy
(256) 544-7604
jim.dowdy@nasa.gov

Stennis Space Center

Ramona Travis
(228) 688-3832
ramona.e.travis@ssc.nasa.gov

NASA Headquarters

Innovative Partnerships Office

Doug Comstock, Director
(202) 358-2221
doug.comstock@nasa.gov

Daniel Lockney,
Technology Transfer Lead
(202) 358-2037
daniel.p.lockney@nasa.gov

Small Business Innovation Research (SBIR) & Small Business Technology Transfer (STTR) Programs

Carl Ray, Program Executive
(202) 358-4652
carl.g.ray@nasa.gov



TECH BRIEFS

NATIONAL AERONAUTICS AND SPACE ADMINISTRATION

5 Technology Focus: Sensors

- 5 Computational Ghost Imaging for Remote Sensing
- 5 Digital Architecture for a Trace Gas Sensor Platform
- 6 Dispersed Fringe Sensing Analysis — DFSA
- 6 Indium Tin Oxide Resistor-Based Nitric Oxide Microsensors
- 7 Gas Composition Sensing Using Carbon Nanotube Arrays
- 7 Sensor for Boundary Shear Stress in Fluid Flow
- 8 Model-Based Method for Sensor Validation

9 Electronics/Computers

- 9 Qualification of Engineering Camera for Long-Duration Deep Space Missions
- 9 Remotely Powered Reconfigurable Receiver for Extreme Environment Sensing Platforms
- 10 Bump Bonding Using Metal-Coated Carbon Nanotubes

11 Software

- 11 In Situ Mosaic Brightness Correction
- 11 Simplex GPS and InSAR Inversion Software
- 11 Virtual Machine Language 2.1
- 12 Multi-Scale Three-Dimensional Variational Data Assimilation System for Coastal Ocean Prediction
- 12 Pandora Operation and Analysis Software

13 Manufacturing & Prototyping

- 13 Fabrication of a Cryogenic Bias Filter for Ultrasensitive Focal Plane
- 13 Processing of Nanosensors Using a Sacrificial Template Approach

15 Materials & Coatings

- 15 High-Temperature Shape Memory Polymers
- 15 Modular Flooring System
- 16 Non-Toxic, Low-Freezing, Drop-In Replacement Heat Transfer Fluids
- 16 Materials That Enhance Efficiency and Radiation Resistance of Solar Cells

17 Mechanics/Machinery

- 17 Low-Cost, Rugged High-Vacuum System
- 17 Static Gas-Charging Plug
- 17 Floating Oil-Spill Containment Device
- 18 Stemless Ball Valve

21 Bio-Medical

- 21 Improving Balance Function Using Low Levels of Electrical Stimulation of the Balance Organs

23 Physical Sciences

- 23 Oxygen-Methane Thruster
- 23 Lunar Navigation Determination System — LaNDS
- 23 Launch Method for Kites in Low-Wind or No-Wind Conditions
- 24 Supercritical CO₂ Cleaning System for Planetary Protection and Contamination Control Applications
- 24 Design and Performance of a Wideband Radio Telescope

27 Information Technology

- 27 Finite Element Models for Electron Beam Freeform Fabrication Process
- 27 Autonomous Information Unit for Fine-Grain Data Access Control and Information Protection in a Net-Centric System
- 28 Vehicle Detection for RCTA/ANS (Autonomous Navigation System)
- 28 Image Mapping and Visual Attention on the Sensory Ego-Sphere
- 29 HyDE Framework for Stochastic and Hybrid Model-Based Diagnosis
- 29 IMAGESEER — IMAGES for Education and Research

This document was prepared under the sponsorship of the National Aeronautics and Space Administration. Neither the United States Government nor any person acting on behalf of the United States Government assumes any liability resulting from the use of the information contained in this document, or warrants that such use will be free from privately owned rights.



Computational Ghost Imaging for Remote Sensing

Ghost imaging is used in encryption, remote sensing, and biomedical imaging applications.

NASA's Jet Propulsion Laboratory, Pasadena, California

This work relates to the generic problem of remote active imaging; that is, a source illuminates a target of interest and a receiver collects the scattered light off the target to obtain an image. Conventional imaging systems consist of an imaging lens and a high-resolution detector array [e.g., a CCD (charge coupled device) array] to register the image. However, conventional imaging systems for remote sensing require high-quality optics and need to support large detector arrays and associated electronics. This results in suboptimal size, weight, and power consumption.

Computational ghost imaging (CGI) is a computational alternative to this traditional imaging concept that has a very simple receiver structure. In CGI, the transmitter illuminates the target with a modulated light source. A single-pixel (bucket) detector collects the scattered light. Then, via computation (i.e., post-processing), the receiver can “reconstruct” the image using the knowledge of the modulation that was projected onto the target by the transmitter. This way, one can construct a very simple receiver that, in principle, requires no lens to image a target.

Ghost imaging is a transverse imaging modality that has been receiving much attention owing to a rich inter-

connection of novel physical characteristics and novel signal processing algorithms suitable for active computational imaging. The original ghost imaging experiments consisted of two correlated optical beams traversing distinct paths and impinging on two spatially-separated photodetectors: one beam interacts with the target and then illuminates on a single-pixel (bucket) detector that provides no spatial resolution, whereas the other beam traverses an independent path and impinges on a high-resolution camera without any interaction with the target. The term “ghost imaging” was coined soon after the initial experiments were reported, to emphasize the fact that by cross-correlating two photocurrents, one generates an image of the target. In CGI, the measurement obtained from the reference arm (with the high-resolution detector) is replaced by a computational derivation of the measurement-plane intensity profile of the reference-arm beam. The algorithms applied to computational ghost imaging have diversified beyond simple correlation measurements, and now include modern reconstruction algorithms based on compressive sensing.

The physical principles underpinning CGI are as follows: the transmitter, by use

of a spatial light modulator, projects a spatiotemporally varying speckle pattern on the target. The scattered light from the target is collected with a simple bucket detector offering no spatial resolution. The photocurrent, whose fluctuations in excess of the shot-noise floor are proportional to the sum of the fluctuations seen in the transmitter-generated speckles, is then processed to resolve the transverse profile of the object. This signal processing can take on a rather elementary linear form such as cross-correlation, or can be more complex and nonlinear, such as L1-norm minimization. The latter form of ghost imaging is known as compressive, as it utilizes techniques developed for compressive imaging. Turbulence near the target has negligible impact on ghost imaging. The most restrictive source of speckle in remote sensing is that induced by the diffuse surface scattering from the target itself. It is evident from earlier analysis that once the speckle is fully developed, no additional gain is possible from integration, and de-correlated speckles must be obtained by using angular, spectral, or polarization diversity.

This work was done by Baris I. Erkmen of Caltech for NASA's Jet Propulsion Laboratory. For more information, contact iaoffice@jpl.nasa.gov. NPO-48157

Digital Architecture for a Trace Gas Sensor Platform

John H. Glenn Research Center, Cleveland, Ohio

A digital architecture has been implemented for a trace gas sensor platform, as a companion to standard analog control electronics, which accommodates optical absorption whose fractional absorbance equivalent would result in excess error if assumed to be linear. In cases where the absorption (1-transmission) is not equivalent to the fractional absorbance within a few percent error, it is necessary to ac-

commodate the actual measured absorption while reporting the measured concentration of a target analyte with reasonable accuracy. This requires incorporation of programmable intelligence into the sensor platform so that flexible interpretation of the acquired data may be accomplished.

Several different digital component architectures were tested and implemented. Commercial off-the-shelf digi-

tal electronics including data acquisition cards (DAQs), complex programmable logic devices (CPLDs), field-programmable gate arrays (FPGAs), and microcontrollers have been used to achieve the desired outcome. The most completely integrated architecture achieved during the project used the CPLD along with a microcontroller. The CPLD provides the initial digital demodulation of the raw sensor signal,

and then communicates over a parallel communications interface with a microcontroller. The microcontroller analyzes the digital signal from the CPLD, and applies a non-linear correction obtained through extensive data analysis at the various relevant EVA operating pressures. The microcontroller then presents the quantitatively accurate carbon dioxide partial pressure regardless of optical density.

This technique could extend the linear dynamic range of typical absorption

spectrometers, particularly those whose low end noise equivalent absorbance is below one-part-in-100,000. In the EVA application, it allows introduction of a path-length-enhancing architecture whose optical interference effects are well understood and quantified without sacrificing the dynamic range that allows quantitative detection at the higher carbon dioxide partial pressures. The digital components are compact and allow reasonably complete integration with separately developed analog control

electronics without sacrificing size, mass, or power draw.

This work was done by Paula Gonzales, Miguel Casias, Andrei Vakhtin, and Jeffrey Pilgrim of Vista Photonics, Inc. for Glenn Research Center. Further information is contained in a TSP (see page 1).

Inquiries concerning rights for the commercial use of this invention should be addressed to NASA Glenn Research Center, Innovative Partnerships Office, Attn: Steven Fedor, Mail Stop 4-8, 21000 Brookpark Road, Cleveland, Ohio 44135. Refer to LEW-18730-1.

Dispersed Fringe Sensing Analysis — DFSA

NASA's Jet Propulsion Laboratory, Pasadena, California

Dispersed Fringe Sensing (DFS) is a technique for measuring and phasing segmented telescope mirrors using a dispersed broadband light image. DFS is capable of breaking the monochromatic light ambiguity, measuring absolute piston errors between segments of large segmented primary mirrors to tens of nanometers accuracy over a range of 100 micrometers or more.

The DFSA software tool analyzes DFS images to extract DFS encoded segment piston errors, which can be used to measure piston distances between primary mirror segments of ground and space telescopes. This information is necessary to control mirror segments to establish a smooth, continuous primary figure needed to achieve high optical quality.

The DFSA tool is versatile, allowing precise piston measurements from a variety of different optical configurations. DFSA technology may be used for meas-

uring wavefront pistons from sub-apertures defined by adjacent segments (such as Keck Telescope), or from separated sub-apertures used for testing large optical systems (such as sub-aperture wavefront testing for large primary mirrors using auto-collimating flats). An experimental demonstration of the coarse-phasing technology with verification of DFSA was performed at the Keck Telescope.

DFSA includes image processing, wavelength and source spectral calibration, fringe extraction line determination, dispersed fringe analysis, and wavefront piston sign determination. The code is robust against internal optical system aberrations and against spectral variations of the source. In addition to the DFSA tool, the software package contains a simple but sophisticated MATLAB model to generate dispersed fringe images of optical system configurations in order to quickly estimate the

coarse phasing performance given the optical and operational design requirements. Combining MATLAB (a high-level language and interactive environment developed by MathWorks), MACOS (JPL's software package for Modeling and Analysis for Controlled Optical Systems), and DFSA provides a unique optical development, modeling and analysis package to study current and future approaches to coarse phasing controlled segmented optical systems.

This work was done by Norbert Sigrist, Fang Shi, David C. Redding, Scott A. Basinger, Catherine M. Ohara, Byoung-Joon Seo, Siddarayappa A. Bikkannavar, and Joshua A. Spechler of Caltech for NASA's Jet Propulsion Laboratory. For more information, contact iaoffice@jpl.nasa.gov.

This software is available for commercial licensing. Please contact Daniel Broderick of the California Institute of Technology at danielb@caltech.edu. Refer to NPO-48019.

Indium Tin Oxide Resistor-Based Nitric Oxide Microsensors

Applications for these sensors include engine emission and environmental monitoring.

John H. Glenn Research Center, Cleveland, Ohio

A sensitive resistor-based NO microsensor, with a wide detection range and a low detection limit, has been developed. Semiconductor microfabrication techniques were used to create a sensor that has a simple, robust structure with a sensing area of 1.10×0.99 mm. A Pt interdigitated structure was used for the electrodes to maximize the sensor signal output. N-type semiconductor indium tin oxide (ITO) thin film was sputter-deposited as a sensing material on the electrode surface, and be-

tween the electrode fingers. Alumina substrate (250 μ m in thickness) was sequentially used for sensor fabrication.

The resulting sensor was tested by applying a voltage across the two electrodes and measuring the resulting current. The sensor was tested at different concentrations of NO-containing gas at a range of temperatures. Preliminary results showed that the sensor had a relatively high sensitivity to NO at 450 °C and 1 V. NO concentrations from ppm to ppb ranges were detected with the

low limit of near 159 ppb. Lower NO concentrations are being tested.

Two sensing mechanisms were involved in the NO gas detection at ppm level: adsorption and oxidation reactions, whereas at ppb level of NO, only one sensing mechanism of adsorption was involved.

The NO microsensor has the advantages of high sensitivity, small size, simple batch fabrication, high sensor yield, low cost, and low power consumption due to its microsize. The resistor-based

thin-film sensor is meant for detection of low concentrations of NO gas, mainly in the ppb or lower range, and is being developed concurrently with other sensor technology for multi-species detection.

This development demonstrates that ITO is a sensitive sensing material for NO detection. It also provides crucial

information for future selection of nanostructured and nanosized NO sensing materials, which are expected to be more sensitive and to consume less power.

This work was done by Jennifer C. Xu and Gary W. Hunter of NASA Glenn Research Center, José M. Gonzalez III of Gilcrest at NASA GRC, and Chung-Chiun

Liu of Case Western Reserve University. Further information is contained in a TSP (see page 1).

Inquiries concerning rights for the commercial use of this invention should be addressed to NASA Glenn Research Center, Innovative Partnerships Office, Attn: Steven Fedor, Mail Stop 4-8, 21000 Brookpark Road, Cleveland, Ohio 44135. Refer to LEW-18782-1.

Gas Composition Sensing Using Carbon Nanotube Arrays

Lightweight sensor provides measurements as accurate as conventional methods.

Ames Research Center, Moffett Field, California

This innovation is a lightweight, small sensor for inert gases that consumes a relatively small amount of power and provides measurements that are as accurate as conventional approaches. The sensing approach is based on generating an electrical discharge and measuring the specific gas breakdown voltage associated with each gas present in a sample.

An array of carbon nanotubes (CNTs) in a substrate is connected to a variable-pulse voltage source. The CNT tips are spaced appropriately from the second electrode maintained at a constant voltage. A sequence of voltage pulses is applied and a pulse discharge breakdown threshold voltage is estimated for one or more gas components, from an analysis of the current-voltage characteristics.

Each estimated pulse discharge breakdown threshold voltage is compared with known threshold voltages for candidate gas components to estimate whether at least one candidate gas component is present in the gas. The procedure can be repeated at higher pulse voltages to estimate a pulse discharge breakdown threshold voltage for a second component present in the gas.

The CNTs in the gas sensor have a sharp (low radius of curvature) tip; they are preferably multiwall carbon nanotubes (MWCNTs) or carbon nanofibers (CNFs), to generate high-strength electrical fields adjacent to the tips for breakdown of the gas components with lower voltage application and generation of high current. The sensor system

can provide a high-sensitivity, low-power-consumption tool that is very specific for identification of one or more gas components. The sensor can be multiplexed to measure current from multiple CNT arrays for simultaneous detection of several gas components.

This work was done by Jing Li and Meyya Meyyappan of Ames Research Center. Further information is contained in a TSP (see page 1).

This invention has been patented by NASA (U.S. Patent No. 7,426,848). Inquiries concerning rights for the commercial use of this invention should be addressed to the Ames Technology Partnerships Division at (650) 604-5238. Refer to ARC-15460-1.

Sensor for Boundary Shear Stress in Fluid Flow

These sensors can be used in automobiles, airplanes, and ocean engineering.

NASA's Jet Propulsion Laboratory, Pasadena, California

The formation of scour patterns at bridge piers is driven by the forces at the boundary of the water flow. In most experimental scour studies, indirect processes have been applied to estimate the shear stress using measured velocity profiles. The estimations are based on theoretical models and associated assumptions. However, the turbulence flow fields and boundary layer in the pier-scour region are very complex and lead to low-fidelity results. In addition, available turbulence models cannot account accurately for the bed roughness effect.

Direct measurement of the boundary shear stress, normal stress, and their fluctuations are attractive alternatives.

However, most direct-measurement shear sensors are bulky in size or not compatible to fluid flow.

A sensor has been developed that consists of a floating plate with folded beam support and an optical grid on the back, combined with a high-resolution optical position probe. The folded beam support makes the floating plate more flexible in the sensing direction within a small footprint, while maintaining high stiffness in the other directions. The floating plate converts the shear force to displacement, and the optical probe detects the plate's position with nanometer resolution by sensing the pattern of the diffraction field of the grid through a glass window. This con-

figuration makes the sensor compatible with liquid flow applications.

Most shear boundary fluid sensors using a direct measurement method include a floating plate and a position sensor. The plate moves under the shear force. To obtain high sensitivity, the floating part of the plate is supported with a structure flexible in the sensing direction and stiff in other directions. The structure could be in plane with the plate or out of plane. The in-plane support structure has an advantage to be fabricated by micromachining technology. The flexible support requires long beams and results in a large footprint. This approach applied a folded beam support to the floating plate design. The

folded beams allow a much smaller footprint to achieve the same flexibility as the conventional configuration.

The breadboard sensor was tested in a water tank testbed. The testbed includes a “false bottom” plate and a running conveyor belt. The false bottom plate simulates the riverbed, and provides an opening for attaching the sensor mounting plate and an air pocket for separating the encoder from the water. The running belt is placed parallel to the direction of measurement, and is placed on a structure different than the false bottom for vibration isolation. The belt was running at controlled speed of up to 2 m/s in both forward

and opposite directions, about 38 mm above the false bottom plate where the sensor was mounted. An average position change is about 620 nm, corresponding to a change in direction of the boundary shear stress. The fluctuation is believed to be caused by the turbulence of the flow.

Another flexure with a 3D configuration was proposed as well. The 3D version was designed to allow for a plate to rotate about an axis defined by three sets of flexures. The plate is mounted on a beam that passes through this axis and extends on the other side of the axis where it has a free end. An optical or capacitive sensor would read the displacement of the free

end of the beam, which would be used with the flexure’s stiffness to calculate the shear force on the sensor plate. This configuration could use the horizontal blade to separate the test media, such as water, from the optical or capacitive sensor, but would present more manufacturing and packaging challenges.

This work was done by Xiaoqi Bao, Mircea Badescu, Stewart Sherrit, Yoseph Bar-Cohen, Shyh-Shiuh Lih, Zensheu Chang, and Brian P. Trease of Caltech; Kornel Kerenyi of the Federal Highway Administration; and Scott E. Widholm and Patrick N. Ostlund of Cal Poly Pomona for NASA’s Jet Propulsion Laboratory. Further information is contained in a TSP (see page 1). NPO-47812

Model-Based Method for Sensor Validation

NASA’s Jet Propulsion Laboratory, Pasadena, California

Fault detection, diagnosis, and prognosis are essential tasks in the operation of autonomous spacecraft, instruments, and *in situ* platforms. One of NASA’s key mission requirements is robust state estimation. Sensing, using a wide range of sensors and sensor fusion approaches, plays a central role in robust state estimation, and there is a need to diagnose sensor failure as well as component failure. Sensor validation can be considered to be part of the larger effort of improving reliability and safety.

The standard methods for solving the sensor validation problem are based on

probabilistic analysis of the system, from which the method based on Bayesian networks is most popular. Therefore, these methods can only predict the most probable faulty sensors, which are subject to the initial probabilities defined for the failures.

The method developed in this work is based on a model-based approach and provides the faulty sensors (if any), which can be logically inferred from the model of the system and the sensor readings (observations). The method is also more suitable for the systems when it is hard, or even impossible, to find the probability functions

of the system. The method starts by a new mathematical description of the problem and develops a very efficient and systematic algorithm for its solution. The method builds on the concepts of analytical redundant relations (ARRs).

This work was done by Farrokh Vatan of Caltech for NASA’s Jet Propulsion Laboratory. Further information is contained in a TSP (see page 1).

The software used in this innovation is available for commercial licensing. Please contact Daniel Broderick of the California Institute of Technology at danielb@caltech.edu. Refer to NPO-47574.



Qualification of Engineering Camera for Long-Duration Deep Space Missions

NASA's Jet Propulsion Laboratory, Pasadena, California

Qualification and verification of advanced electronic packaging and interconnect technologies, and various other types of hardware elements for the Mars Exploration Rover's Spirit and Opportunity (MER)/Mars Science Laboratory (MSL) flight projects, has been performed to enhance the mission assurance. The qualification of hardware (engineering camera) under extreme cold temperatures has been performed with reference to various Mars-related project requirements. The flight-like packages, sensors, and subassemblies have been selected for the study to survive three times the total number of expected diurnal temperature cycles resulting from all environmental and operational expo-

sure occurring over the life of the flight hardware, including all relevant manufacturing, ground operations, and mission phases.

Qualification has been performed by subjecting above flight-like hardware to the environmental temperature extremes, and assessing any structural failures or degradation in electrical performance due to either overstress or thermal cycle fatigue.

Engineering camera packaging designs, charge-coupled devices (CCDs), and temperature sensors were successfully qualified for MER and MSL per JPL design principles. Package failures were observed during qualification processes and the package redesigns were then

made to enhance the reliability and subsequent mission assurance. These results show the technology certainly is promising for MSL, and especially for long-term extreme temperature missions to the extreme temperature conditions.

The engineering camera has been completely qualified for the MSL project, with the proven ability to survive on Mars for 2010 sols, or 670 sols times three. Finally, the camera continued to be functional, even after 2010 thermal cycles.

This work was done by Rajeshuni Ramesham, Justin N. Maki, Ali M. Pourangi, and Steven W. Lee of Caltech for NASA's Jet Propulsion Laboratory. For more information, contact iaoffice@jpl.nasa.gov. NPO-47666

Remotely Powered Reconfigurable Receiver for Extreme Environment Sensing Platforms

This receiver also can be used in harsh environments encountered in aerospace and mining.

NASA's Jet Propulsion Laboratory, Pasadena, California

Wireless sensors connected in a local network offer revolutionary exploration capabilities, but the current solutions do not work in extreme environments of low temperatures (200K) and low to moderate radiation levels (<50 krad). These sensors (temperature, radiation, infrared, etc.) would need to operate outside the spacecraft/lander and be totally independent of power from the spacecraft/lander. Flash memory field-programmable gate arrays (FPGAs) are being used as the main signal processing and protocol generation platform in a new receiver. Flash-based FPGAs have been shown to have at least 100× reduced standby power and 10× reduction operating power when compared to normal SRAM-based FPGA technology.

Supercapacitors are nanotechnology-based electrochemical capacitors that can be cycled millions of times, com-

pared to tens to hundreds of times for batteries. This allows supercapacitors to be used in conjunction with batteries by acting as a charge conditioner, storing energy for load-balancing purposes and then using any excess energy to charge the batteries at a suitable time. Supercapacitors are insensitive to radiation past 1 Mrad. JPL has demonstrated supercapacitor electrolytes that function to 189K.

This technology uses the ultra-low-power flash-based FPGA as the communication protocol (physical and medium layers) generator that is powered by a hybrid combination of lithium-based batteries and supercapacitors. A SiGe based RF front end can be used to provide transmitter/receiver capability for the 2.45-GHz and 858-MHz ISM frequency bands at low temperatures. The low power is critical because it defines how long the system can operate. The cold temperatures will reduce the performance of the

batteries. Instead of lasting a year at room temperature, a lithium battery may only last a few weeks at cold temperatures. Even at cold temperatures, the battery output will be reduced. This means only a very-low-power circuit can be considered for use. The supercapacitors provide additional direct power capability for short-burst communication, and they provide the ability to extend the life of the battery by maintaining the voltage longer than the battery could alone. The FPGA can implement load-balancing and control logic to enable the battery to either operate completely alone, in combination with the supercapacitors, or have the supercapacitors alone power the FPGA in standby mode and/or be the startup power source if the FPGA is completely powered off.

This powering-off capability exists due to the use of the non-volatile flash memory cell-based FPGAs. This allows the su-

percapacitor to act also in countdown circuit mode, where the discharge time constant of the circuit is used as the time to keep the FPGA power off in order to save power. Once the supercapacitor-based circuit reaches a given level, this voltage is sensed and the wake-up sequence to the FPGA begins.

The supercapacitors also provide the ability to store and harvest recharge energy for the battery. RF energy can be beamed into the system and then fed back into the battery/supercapacitor

network. Alternatively, mechanical energy from a MEMS device can be used to re-charge the supercapacitor. The capacitors can be quickly charged up and then act as a power reservoir for the battery. The completely described system above is currently in development.

This work was done by Douglas J. Sheldon of Caltech for NASA's Jet Propulsion Laboratory. Further information is contained in a TSP (see page 1).

In accordance with Public Law 96-517, the contractor has elected to retain title to this

invention. Inquiries concerning rights for its commercial use should be addressed to:

*Innovative Technology Assets Management
JPL*

Mail Stop 202-233

4800 Oak Grove Drive

Pasadena, CA 91109-8099

E-mail: iaoffice@jpl.nasa.gov

Refer to NPO-47718, volume and number of this NASA Tech Briefs issue, and the page number.

Bump Bonding Using Metal-Coated Carbon Nanotubes

NASA's Jet Propulsion Laboratory, Pasadena, California

Bump bonding hybridization techniques use arrays of indium bumps to electrically and mechanically join two chips together. Surface-tension issues limit bump sizes to roughly as wide as they are high. Pitches are limited to 50 microns with bumps only 8–14 microns high on each wafer. A new process uses oriented carbon nanotubes (CNTs) with a metal (indium) in a wicking process using capillary actions to increase the aspect ratio and pitch density of the connections for bump bonding hybridizations. It merges the properties of the CNTs and the metal bumps, providing enhanced material performance parameters.

By merging the bumps with narrow and long CNTs oriented in the vertical direction, higher aspect ratios can be obtained if the metal can be made to wick. Possible aspect ratios increase from 1:1 to 20:1 for most applications, and to 100:1 for some applications. Possible pitch density increases of a factor of 10 are possible.

Standard capillary theory would not normally allow indium or most other metals to be drawn into the oriented CNTs, because they are non-wetting. However, capillary action can be induced through the ability to fabricate oriented CNT bundles to desired spacings, and the use of deposition tech-

niques and temperature to control the size and mobility of the liquid metal streams and associated reservoirs.

This hybridization of two technologies (indium bumps and CNTs) may also provide for some additional benefits such as improved thermal management and possible current density increases.

This work was done by James L. Lamb, Matthew R. Dickie, Robert S. Kowalczyk, and Anna Liao of Caltech; and Michael J. Bronikowski of Atomate Corporation for NASA's Jet Propulsion Laboratory. Further information is contained in a TSP (see page 1). NPO-46592



In Situ Mosaic Brightness Correction

In situ missions typically have pointable, mast-mounted cameras, which are capable of taking panoramic mosaics comprised of many individual frames. These frames are mosaicked together. While the mosaic software applies radiometric correction to the images, in many cases brightness/contrast seams still exist between frames. This is largely due to errors in the radiometric correction, and the absence of correction for photometric effects in the mosaic processing chain. The software analyzes the overlaps between adjacent frames in the mosaic and determines correction factors for each image in an attempt to reduce or eliminate these brightness seams.

Two related methods of correcting brightness differences at seams between frames in a mosaic of *in situ* images work on the same general principle. The overlapping areas between adjacent frames in a mosaic are analyzed, and statistics are gathered. These statistics are then used in a bundle-adjustment style procedure to derive correction parameters for each image that minimize the brightness seams across the mosaic.

The older method consists of two programs: marsint, which gathers overlap statistics, and marsbias, which determines correction parameters. The newer system adds additional capabilities, including simultaneous brightness and contrast correction, better overlap statistics, improved image labels, and standard XML file formats. The overlap analysis functionality is embedded in the mosaic program marsmap, while the correction parameters are determined by the program marsbrt.

In both cases, the correction parameters are input to the mosaic program of interest (marsmap, marsmos, marsm-cauley) to be applied to the mosaic. Correction parameters are constant additive or multiplicative factors applied to the entire input image; no nonlinear corrections are applied.

The software is part of the OPGS (Operational Product Generation Subsystem) software suite. While the algorithms behind this suite are not particularly unique, what makes the programs useful is their integration into the larger *in situ* image processing system via the PIG library and the

mosaic programs. They work directly with space *in situ* data, understanding the appropriate image metadata fields and updating them properly.

This work was done by Robert G. Deen and Jean J. Lorre of Caltech for NASA's Jet Propulsion Laboratory. For more information, contact iaoffice@jpl.nasa.gov. NPO-47726

Simplex GPS and InSAR Inversion Software

Changes in the shape of the Earth's surface can be routinely measured with precisions better than centimeters. Processes below the surface often drive these changes and as a result, investigators require models with inversion methods to characterize the sources. Simplex inverts any combination of GPS (global positioning system), UAVSAR (uninhabited aerial vehicle synthetic aperture radar), and InSAR (interferometric synthetic aperture radar) data simultaneously for elastic response from fault and fluid motions. It can be used to solve for multiple faults and parameters, all of which can be specified or allowed to vary. The software can be used to study long-term tectonic motions and the faults responsible for those motions, or can be used to invert for co-seismic slip from earthquakes. Solutions involving estimation of fault motion and changes in fluid reservoirs such as magma or water are possible. Any arbitrary number of faults or parameters can be considered.

Simplex specifically solves for any of location, geometry, fault slip, and expansion/contraction of a single or multiple faults. It inverts GPS and InSAR data for elastic dislocations in a half-space. Slip parameters include strike slip, dip slip, and tensile dislocations. It includes a map interface for both setting up the models and viewing the results. Results, including faults, and observed, computed, and residual displacements, are output in text format, a map interface, and can be exported to KML. The software interfaces with the QuakeTables database allowing a user to select existing fault parameters or data. Simplex can be accessed through the QuakeSim portal graphical user interface or run from a UNIX command line.

This work was done by Andrea Donnellan, Jay W. Parker, and Gregory A. Lyzenga of

Caltech, and Marlon E. Pierce of Indiana University for NASA's Jet Propulsion Laboratory. For more information, contact iaoffice@jpl.nasa.gov.

This software is available for commercial licensing. Please contact Daniel Broderick of the California Institute of Technology at danielb@caltech.edu. Refer to NPO-48233.

Virtual Machine Language 2.1

VML (Virtual Machine Language) is an advanced computing environment that allows spacecraft to operate using mechanisms ranging from simple, time-oriented sequencing to advanced, multi-component reactive systems.

VML has developed in four evolutionary stages. VML 0 is a core execution capability providing multi-threaded command execution, integer data types, and rudimentary branching. VML 1 added named parameterized procedures, extensive polymorphism, data typing, branching, looping issuance of commands using run-time parameters, and named global variables. VML 2 added for loops, data verification, telemetry reaction, and an open flight adaptation architecture. VML 2.1 contains major advances in control flow capabilities for executable state machines.

On the resource requirements front, VML 2.1 features a reduced memory footprint in order to fit more capability into modestly sized flight processors, and endian-neutral data access for compatibility with Intel little-endian processors. Sequence packaging has been improved with object-oriented programming constructs and the use of implicit (rather than explicit) time tags on statements. Sequence event detection has been significantly enhanced with multi-variable waiting, which allows a sequence to detect and react to conditions defined by complex expressions with multiple global variables. This multi-variable waiting serves as the basis for implementing parallel rule checking, which in turn, makes possible executable state machines.

The new state machine feature in VML 2.1 allows the creation of sophisticated autonomous reactive systems without the need to develop expensive flight software. Users specify named states and transitions, along with the truth conditions required, before taking transitions. Transi-

tions with the same signal name allow separate state machines to coordinate actions: the conditions distributed across all state machines necessary to arm a particular signal are evaluated, and once found true, that signal is raised. The selected signal then causes all identically named transitions in all present state machines to be taken simultaneously.

VML 2.1 has relevance to all potential space missions, both manned and unmanned. It was under consideration for use on Orion.

This work was done by Joseph E. Riedel of Caltech and Christopher A. Grasso of Blue Sun Enterprises for NASA's Jet Propulsion Laboratory. Further information is contained in a TSP (see page 1).

This software is available for commercial licensing. Please contact Daniel Broderick of the California Institute of Technology at danielb@caltech.edu. Refer to NPO-47696.

Multi-Scale Three-Dimensional Variational Data Assimilation System for Coastal Ocean Prediction

A multi-scale three-dimensional variational data assimilation system (MS-3DVAR) has been formulated and the associated software system has been developed for improving high-resolution coastal ocean prediction. This system helps improve coastal ocean prediction skill, and has been used in support of operational coastal ocean forecasting systems and field experiments. The sys-

tem has been developed to improve the capability of data assimilation for assimilating, simultaneously and effectively, sparse vertical profiles and high-resolution remote sensing surface measurements into coastal ocean models, as well as constraining model biases.

In this system, the cost function is decomposed into two separate units for the large- and small-scale components, respectively. As such, data assimilation is implemented sequentially from large to small scales, the background error covariance is constructed to be scale-dependent, and a scale-dependent dynamic balance is incorporated. This scheme then allows effective constraining large scales and model bias through assimilating sparse vertical profiles, and small scales through assimilating high-resolution surface measurements.

This MS-3DVAR enhances the capability of the traditional 3DVAR for assimilating highly heterogeneously distributed observations, such as along-track satellite altimetry data, and particularly maximizing the extraction of information from limited numbers of vertical profile observations.

This work was done by Zhijin Li, Yi Chao, and P. Peggy Li of Caltech for NASA's Jet Propulsion Laboratory. For more information, contact iaoffice@jpl.nasa.gov.

This software is available for commercial licensing. Please contact Daniel Broderick of the California Institute of Technology at danielb@caltech.edu. Refer to NPO-47768.

Pandora Operation and Analysis Software

Pandora Operation and Analysis Software controls the Pandora Sun- and sky-pointing optical head and built-in filter wheels (neutral density, UV bandpass, polarization filters, and opaque). The software also controls the attached spectrometer exposure time and thermoelectric cooler to maintain the spectrometer temperature to within 1 °C. All functions are available through a GUI so as to be easily accessible by the user. The data are automatically stored on a miniature computer (netbook) for automatic download to a designated server at user defined intervals (once per day, once per week, etc.), or to a USB external device. An additional software component reduces the raw data (spectrometer counts) to preliminary scientific products for quick-view purposes. The Pandora systems are built from off-the-shelf commercial parts and from mechanical parts machined using electronic machine shop drawings. The Pandora spectrometer system is designed to look at the Sun (tracking to within 0.1°), or to look at the sky at any zenith or azimuth angle, to gather information about the amount of trace gases or aerosols that are present.

This work was done by Jay Herman, Alexander Cede, and Nader Abuhassan of the University of Maryland for Goddard Space Flight Center. Further information is contained in a TSP (see page 1). GSC-16080-1



Fabrication of a Cryogenic Bias Filter for Ultrasensitive Focal Plane

Goddard Space Flight Center, Greenbelt, Maryland

A fabrication process has been developed for cryogenic in-line filtering for the bias and readout of ultrasensitive cryogenic bolometers for millimeter and submillimeter wavelengths. The design is a microstripline filter that cuts out, or strongly attenuates, frequencies (10–50 GHz) that can be carried by wiring staged at cryogenic temperatures. The filter must have 100-percent transmission at DC and low frequencies where the bias and readout lines will carry signal. The fabrication requires the encapsulation of superconducting wiring in a dielectric-metal envelope with precise electrical characteristics. Sufficiently thick insulation layers with high-conductivity metal layers fully surrounding a patterned su-

perconducting wire in arrayable formats have been demonstrated.

A degenerately doped silicon wafer has been chosen to provide a metallic ground plane. A metallic seed layer is patterned to enable attachment to the ground plane. Thick silicon dioxide films are deposited at low temperatures to provide tunable dielectric isolation without degrading the metallic seed layer. Superconducting wiring is deposited and patterned using microstripline filtering techniques to cut out the relevant frequencies. A low T_c superconductor is used so that it will attenuate power strongly above the gap frequency. Thick dielectric is deposited on top of the circuit, and then vias are pat-

terned through both dielectric layers. A thick conductive film is deposited conformally over the entire circuit, except for the contact pads for the signal and bias attachments to complete the encapsulating ground plane. Filters are high-aspect-ratio rectangles, allowing close packing in one direction, while enabling the chip to feed through the wall of a copper enclosure. The chip is secured in the copper wall using a soft metal seal to make good thermal and electrical contact to the outer shield.

This work was done by James Chervenak, Ari Brown, and Edward Wollack of Goddard Space Flight Center. Further information is contained in a TSP (see page 1). GSC-16130-1

Processing of Nanosensors Using a Sacrificial Template Approach

This technique can be applied to a variety of applications, including leak detection, personal health monitoring, and environmental monitoring.

John H. Glenn Research Center, Cleveland, Ohio

A new microsensor fabrication approach has been demonstrated based upon the use of nanostructures as templates. The fundamental idea is that existing nanostructures, such as carbon nanotubes or biological structures, have a material structure that can be used advantageously in order to provide new sensor systems but lack the advantages of some materials to, for example, operate at high temperatures.

The approach is to start with a template using nanostructures such as a carbon nanotube. This template can then be coated by an oxide material with higher temperature capabilities. Upon heating in air, the carbon nanotube template is burned off, leaving only the metal oxide nanostructure. The resulting structure has a combination of the crystal structure and surface morphology of the carbon nanotube, combined with the material durability and high-temperature-sensing properties of the metal oxide. Further, since the metal

oxide nanocrystals are deposited on the carbon nanotube, after burn-off what is left is a metal oxide porous nanostructure. This makes both the interior and the exterior of this nanostructured sensor available for gas species detection. This, in effect, increases the surface area available for sensing, which has been shown in the past to significantly increase sensor performance.

There are a number of advantages to improving the capabilities of sensor materials such as metal oxides. For example, gas sensors based on polycrystalline tin oxide offer many advantages over current technologies for detecting reducing gases, such as low cost, long lifetime, and high selectivity and sensitivity. In general, a major emphasis of research is to produce sensors that are small in size, easy to batch-fabricate, and feature low power consumption.

The fabrication of these microsensors includes three major steps: (1) synthesis of the porous metal or metal oxide

nanotubes using a sacrificial template, (2) deposition of the electrodes onto alumina substrates, and (3) alignment of the nanotubes between the electrodes. This invention was reduced to practice using tin oxide nanotubes while using carbon nanotubes as the template.

A room-temperature methane microsensor based on porous tin oxide nanotubes has been developed using carbon nanotubes as templates. The sensor was fabricated integrating microfabrication techniques with the alignment of the nanostructures. The sensor was operated at room temperature, and detection of 0.25% methane in air was demonstrated. The room-temperature methane microsensor has the advantages of low power consumption, small size, simple to batch-fabricate, and is high in sensor yield.

The room-temperature methane microsensors developed have two major unique and novel attributes. First is the use of the microfabrication process to fabricate microsized sensor electrodes.

The application of photolithography and sputtering processing to fabricate sensor electrodes enables the sensor to have small sizes. The electrodes consist of a sawtooth pattern, which would be very difficult to make with other processes. The electrodes are batch-fabricated with low-cost, high-yield, and robust structure. Second is the use of porous tin oxide nanotubes and the unique design of the sensor structure. By having sawtooth patterned electrodes, the use of dielectrophoresis to align the nanostructures becomes more feasible. Dielectrophoresis exploits the dielectric difference between the solvent and the nanostructures in the solvent to induce temporary dipoles that align with the imposed electric field. The electric field is

greater at the tips of the sawtooth electrodes, which accounts for the preferential alignment of the nanotubes between the tips of opposing sawtooth electrodes.

The technology takes advantage of the structural and morphological properties of lower-temperature sensing materials, and uses them as templates for the formation of sensors with improved durability and temperature range. This approach specifically targets template materials demonstrated for their own ability to detect chemical species. In principle, any material that has advantageous sensor properties and is eliminated through higher-temperature processing can be used as a template. For example, biological materials that have a surface morphology designed for se-

lected detection of chemical species can serve as templates in this process. Thus, a biological material that inherently has structural and morphological properties that facilitate the detection of other species, such as carbon dioxide, can be used as a template to potentially improve the sensing properties of a metal oxide or metal.

This work was done by Azlin M. Biaggi-Labiosa and Gary W. Hunter of Glenn Research Center. Further information is contained in a TSP (see page 1).

Inquiries concerning rights for the commercial use of this invention should be addressed to NASA Glenn Research Center, Innovative Partnerships Office, Attn: Steven Fedor, Mail Stop 4-8, 21000 Brookpark Road, Cleveland, Ohio 44135. Refer to LEW-18768-1.



High-Temperature Shape Memory Polymers

The shape memory behavior is provided by a non-polymer additive.

John H. Glenn Research Center, Cleveland, Ohio

Shape memory materials undergo physical conformation changes when exposed to an external stimulus, such as a change in temperature. Such materials have a permanent shape, but can be reshaped above a critical temperature and fixed into a temporary shape when cooled under stress to below the critical temperature. When reheated above the critical temperature (T_c , also sometimes called the triggering or switching temperature), the materials revert to the permanent shape.

The current innovation involves a chemically treated (sulfonated, carboxylated, phosphonated, or other polar function group), high-temperature, semicrystalline thermoplastic poly(ether ether ketone) ($T_g \approx 140^\circ\text{C}$, $T_m = 340^\circ\text{C}$) mix containing organometallic complexes (Zn^{++} , Li^+ , or other metal, ammonium, or phosphonium salts), or high-temperature ionic liquids (e.g. hexafluorosilicate salt with 1-propyl-3-methyl imidazolium, $T_m = 210^\circ\text{C}$) to form a network where dipolar or ionic

interactions between the polymer and the low-molecular-weight or inorganic compound forms a complex that provides a physical crosslink. Hereafter, these compounds will be referred to as “additives.” The polymer is semicrystalline, and the high-melt-point crystals provide a temporary crosslink that acts as a permanent crosslink just so long as the melting temperature is not exceeded. In this example case, the melting point is $\approx 340^\circ\text{C}$, and the shape memory critical temperature is between 150 and 250°C . PEEK is an engineering thermoplastic with a high Young’s modulus, nominally 3.6 GPa .

An important aspect of the invention is the control of the PEEK functionalization (in this example, the sulfonation degree), and the thermal properties (i.e. melting point) of the additive, which determines the switching temperature. Because the compound is thermoplastic, it can be formed into the “permanent” shape by conventional plastics processing operations. In addition, the

compound may be covalently crosslinked after forming the permanent shape by S-PEEK by applying ionizing radiation (γ radiation, neutrons), or by chemical crosslinking to form a covalent permanent network.

With respect to other shape memory polymers, this invention is novel in that it describes the use of a thermoplastic composition that can be thermally molded or solution-cast into complex “permanent” shapes, and then reheated or redissolved and recast from solution to prepare another shape. It is also unique in that the shape memory behavior is provided by a non-polymer additive.

This work was done by Mitra Yoonessi of Glenn Research Center and Robert A. Weiss of the University of Akron. Further information is contained in a TSP (see page 1).

Inquiries concerning rights for the commercial use of this invention should be addressed to NASA Glenn Research Center, Innovative Partnerships Office, Attn: Steven Fedor, Mail Stop 4-8, 21000 Brookpark Road, Cleveland, Ohio 44135. Refer to LEW-18756-1.

Modular Flooring System

Lighter material is easier to transport and assemble.

Goddard Space Flight Center, Greenbelt, Maryland

The modular flooring system (MFS) was developed to provide a portable, modular, durable carpeting solution for NASA’s Robotics Alliance Project’s (RAP) outreach efforts. It was also designed to improve and replace a modular flooring system that was too heavy for safe use and transportation. The MFS was developed for use as the flooring for various robotics competitions that RAP utilizes to meet its mission goals. One of these competitions, the FIRST Robotics Competition (FRC), currently uses two massive rolls of broadloom carpet for the foundation of the arena in which the robots are contained during the competition. The area of the arena is approximately 30 by

72 ft (≈ 9 by 22 m). This carpet is very cumbersome and requires large-capacity vehicles, and handling equipment and personnel to transport and deploy. The broadloom carpet sustains severe abuse from the robots during a regular three-day competition, and as a result, the carpet is not used again for competition. Similarly, broadloom carpets used for trade shows at convention centers around the world are typically discarded after only one use. This innovation provides a green solution to this wasteful practice.

Each of the flooring modules in the previous system weighed 44 lb ($\approx 20\text{ kg}$). The improvements in the overall design of the system reduce the weight

of each module by approximately 22 lb ($\approx 10\text{ kg}$) (50%), and utilize an improved “module-to-module” connection method that is superior to the previous system.

The MFS comprises 4-by-4-ft ($\approx 1.2\text{-by-1.2-m}$) carpet module assemblies that utilize commercially available carpet tiles that are bonded to a lightweight substrate. The substrate surface opposite from the carpeted surface has a module-to-module connecting interface that allows for the modules to be connected, one to the other, as the modules are constructed. This connection is hidden underneath the modules, creating a smooth, co-planar flooring surface. The modules are stacked and strapped

onto durable, commercially available drywall carts for storage and/or transportation. This method of storage and transportation makes it very convenient

and safe when handling large quantities of modules.

This work was done by Robert Thate of Goddard Space Flight Center. For further in-

formation, contact the Goddard Innovative Partnerships Office at (301) 286-5810. GSC-16240-1

Non-Toxic, Low-Freezing, Drop-In Replacement Heat Transfer Fluids

Lyndon B. Johnson Space Center, Houston, Texas

A non-toxic, non-flammable, low-freezing heat transfer fluid is being developed for drop-in replacement within current and future heat transfer loops currently using water or alcohol-based coolants. Numerous water-soluble compounds were down-selected and screened for toxicological, physical, chemical, compatibility, thermodynamic, and heat transfer properties. Two fluids were developed, one with a freezing point near 0 °C, and one with a suppressed freezing point. Both fluids contain an additive

package to improve material compatibility and microbial resistance.

The optimized sub-zero solution had a freezing point of -30 °C, and a freezing volume expansion of 10-percent of water. The toxicity of the solutions was experimentally determined as LD₅₀ > 5g/kg. The solutions were found to produce “minimal” corrosion with materials identified by NASA as potentially existing in secondary cooling loops.

Thermal/hydrodynamic performance exceeded that of glycol-based fluids with

comparable freezing points for temperatures $T_f < 20^\circ\text{C}$. The additive package was demonstrated as a buffering agent to compensate for CO₂ absorption, and to prevent microbial growth. The optimized solutions were determined to have physically/chemically stable shelf lives for freeze/thaw cycles and long-term test loop tests.

This work was done by J. Michael Cutbirth of Mainstream Engineering Corp. for Johnson Space Center. Further information is contained in a TSP (see page 1). MSC-24547-1

Materials That Enhance Efficiency and Radiation Resistance of Solar Cells

John H. Glenn Research Center, Cleveland, Ohio

A thin layer (≈10 microns) of a novel “transparent” fluorescent material is applied to existing solar cells or modules to effectively block and convert UV light, or other lower solar response waveband of solar radiation, to visible or IR light that can be more efficiently used by solar cells for additional photocurrent. Meanwhile, the layer of fluorescent coating material remains fully “transparent” to the visible and IR waveband of solar radiation, resulting in a net gain of solar cell efficiency.

This innovation alters the effective solar spectral power distribution to which an existing cell gets exposed, and matches the maximum photovoltaic (PV) response of existing cells. By shifting a low PV response waveband (e.g.,

UV) of solar radiation to a high PV response waveband (e.g. Vis-Near IR) with novel fluorescent materials that are transparent to other solar-cell sensitive wavebands, electrical output from solar cells will be enhanced.

This approach enhances the efficiency of solar cells by converting UV and high-energy particles in space that would otherwise be wasted to visible/IR light. This innovation is a generic technique that can be readily implemented to significantly increase efficiencies of both space and terrestrial solar cells, without incurring much cost, thus bringing a broad base of economical, social, and environmental benefits.

The key to this approach is that the “fluorescent” material must be very effi-

cient, and cannot block or attenuate the “desirable and unconverted” waveband of solar radiation (e.g. Vis-NIR) from reaching the cells. Some nano-phosphors and novel organometallic complex materials have been identified that enhance the energy efficiency on some state-of-the-art commercial silicon and thin-film-based solar cells by over 6%.

This work was done by Xiadong Sun and Haorong Wang of Sun Innovations, Inc. for Glenn Research Center. Further information is contained in a TSP (see page 1).

Inquiries concerning rights for the commercial use of this invention should be addressed to NASA Glenn Research Center, Innovative Partnerships Office, Attn: Steven Fedor, Mail Stop 4-8, 21000 Brookpark Road, Cleveland, Ohio 44135. Refer to LEW-18781-1.



❁ Low-Cost, Rugged High-Vacuum System

Goddard Space Flight Center, Greenbelt, Maryland

A need exists for miniaturized, rugged, low-cost high-vacuum systems. Recent advances in sensor technology have led to the development of very small mass spectrometer detectors as well as other analytical instruments such as scanning electron microscopes. However, the vacuum systems to support these sensors remain large, heavy, and power-hungry. To meet this need, a miniaturized vacuum system was developed based on a very small, rugged, and inexpensive-to-manufacture molecular drag pump (MDP). The MDP is enabled by a miniature, very-high-speed (200,000 rpm), rugged, low-power, brushless DC motor optimized for wide temperature operation and long life.

The key advantages of the pump are reduced cost and improved ruggedness compared to other mechanical high-vacuum pumps. The machining of the

rotor and stators is very simple compared to that necessary to fabricate rotor and stator blades for other pump designs. Also, the symmetry of the rotor is such that dynamic balancing of the rotor will likely not be necessary. Finally, the number of parts in the unit is cut by nearly a factor of three over competing designs. The new pump forms the heart of a complete vacuum system optimized to support analytical instruments in terrestrial applications and on spacecraft and planetary landers.

The MDP achieves high vacuum coupled to a ruggedized diaphragm rough pump. Instead of the relatively complicated rotor and stator blades used in turbomolecular pumps, the rotor in the MDP consists of a simple, smooth cylinder of aluminum. This will turn at approximately 200,000 rpm inside an outer stator housing. The pump stator

comprises a cylindrical aluminum housing with one or more specially designed grooves that serve as flow channels. To minimize the length of the pump, the gas is forced down the flow channels of the outer stator to the base of the pump. The gas is then turned and pulled toward the top through a second set of channels cut into an inner stator housing that surrounds the motor. The compressed gas then flows down channels in the motor housing to the exhaust port of the pump. The exhaust port of the pump is connected to a commercially available diaphragm or scroll pump.

This work was done by Paul Sorensen and Robert Kline-Schoder of Creare Inc. for Goddard Space Flight Center. Further information is contained in a TSP (see page 1). GSC-15838-1

❁ Static Gas-Charging Plug

Lyndon B. Johnson Space Center, Houston, Texas

A gas-charging plug can be easily analyzed for random vibration. The design features two steeped O-rings in a radial configuration at two different diameters, with a 0.050-in. (≈ 1.3 -mm) diameter through-hole between the two O-rings. In the charging state, the top O-ring is engaged and sealing. The bottom O-ring outer diameter is not squeezed, and al-

lows air to flow by it into the tank. The inner diameter is stretched to plug the gland diameter, and is restrained by the O-ring groove.

The charging port bushing provides mechanical stop to restrain the plug during gas charge removal. It also prevents the plug from becoming a projectile when removing gas charge from the accumulator.

The plug can easily be verified after installation to ensure leakage requirements are met.

This work was done by William Indoe of Johnson Space Center. For further information, contact the JSC Innovation Partnerships Office at (281) 483-3809. MSC-25059-1

❁ Floating Oil-Spill Containment Device

This triangular device can be used for oil and natural gas containment.

NASA's Jet Propulsion Laboratory, Pasadena, California

Previous oil containment booms have an open top that allows natural gas to escape, and have significant oil leakage due to wave action. Also, a subsea pyramid oil trap exists, but cannot move relative to moving oil plumes from deep-sea oil leaks.

The solution is to have large, moveable oil traps. One version floats on the sea surface and has a flexible tarp cover and a lower weighted skirt to completely entrap the floating oil and natural gas. The device must have at least three sides with boats pulling at each apex, and

sonar or other system to track the slowly moving oil plume, so that the boats can properly locate the booms. The oil trap device must also have a means for removal of the oil and the natural gas.

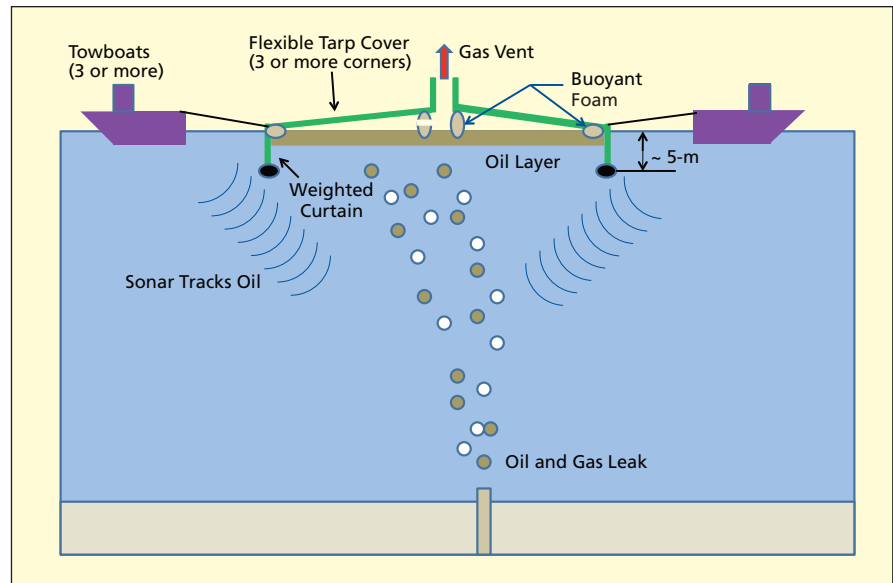
A second design version has a flexible pyramid cover that is attached by lines to

ballast on the ocean floor. This is similar to fixed, metal pyramid oil capture devices in the Santa Barbara Channel off the coast of California. The ballast lines for the improved design, however, would have winches that can move the pyramid to always be located above the oil and gas plume.

A third design is a combination of the first two. It uses a submerged pyramid to trap oil, but has no anchor and uses boats to locate the trap. It has ballast weights located along the bottom of the tarp and/or at the corners of the trap.

The improved floating oil-spill containment device has a large floating boom and weighted skirt surrounding the oil and gas entrapment area. The device is triangular (or more than three sides) and has a flexible tarp cover with a raised gas vent area. Boats pull on the apex of the triangles to maintain tension and to allow the device to move to optimum locations to trap oil and gas. The gas is retrieved from a higher buoyant part of the tarp, and oil is retrieved from the floating oil layer contained in the device.

These devices can be operated in relatively severe weather, since waves will



An Improved Floating Oil-Spill Containment Device features a flexible tarp cover with three or more corners that is pulled by three or more towboats.

break over the devices without causing oil leaking. Also, natural gas is entrapped and can be retrieved. All designs can use sonar to locate the moving oil plume, and then be relocated by using boats or winches to move the oil trapping devices. These devices can be constructed of

treated, non-permeable DuPont Kevlar cloth (or similar material).

This work was done by Jack A. Jones of Caltech for NASA's Jet Propulsion Laboratory. Further information is contained in a TSP (see page 1). NPO47679

Stemless Ball Valve

Potential applications include hazardous fluids and chemicals, and where fugitive emissions from valves are a concern.

Lyndon B. Johnson Space Center, Houston, Texas

This invention utilizes a new method of opening and closing a ball valve. Instead of rotating the ball with a perpendicular stem (as is the case with standard ball valves), the ball is rotated around a fixed axis by two guide pins. This innovation eliminates the leak point that is present in all standard ball valves due to the penetration of an actuation stem through the valve body.

The VOST (Venturi Off-Set-Technology) valve has been developed for commercial applications. The standard version of the valve consists of an off-set venturi flow path through the valve. This path is split at the narrowest portion of the venturi, allowing the section upstream from the venturi to be rotated. As this rotation takes place, the venturi becomes restricted as one face rotates with respect to the other, eventually closing off the flow path. A spring-loaded seal made of resilient material is

embedded in the upstream face of the valve, making a leak-proof seal between the faces; thus a valve is formed. The spring-loaded lip seal is the only seal that can provide a class six, or "bubbletight," seal against the opposite face of the valve. Tearing action of the seal by high-velocity gas on this early design required relocation of the seal to the downstream face of the valve.

In the "stemless" embodiment of this valve, inner and outer magnetic cartridges are employed to transfer mechanical torque from the outside of the valve to the inside without the use of a stem. This eliminates the leak path caused by the valve stems in standard valves because the stems penetrate through the bodies of these valves.

This design requires high precision during assembly for proper performance of the face seal. Slight variations in tolerances result in unacceptable seal

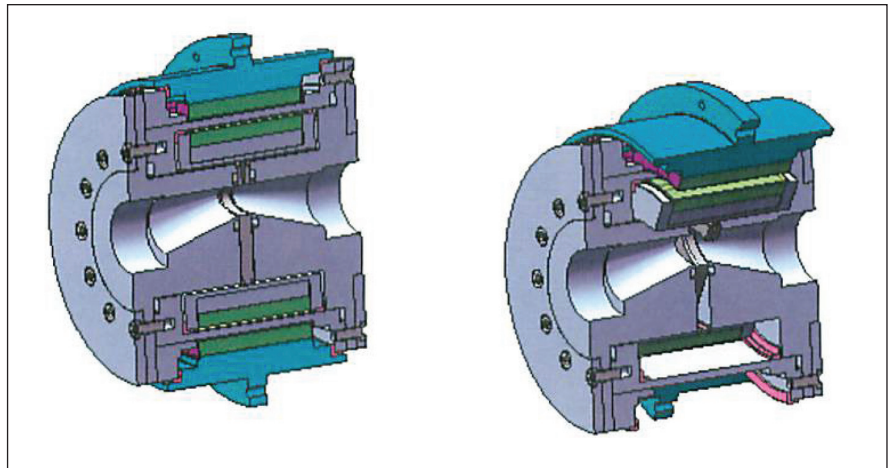
performance. An effort was made to replace this design with a less demanding arrangement of component parts. A rotating gate was proposed to be installed between the two faces of the valve. This gate would rotate in and out of the flow path of the venturi, opening and closing the valve. Although this new gate design would require a seal on both sides of the gate, it would eliminate the requirement of rotating the entire downstream side of the valve. This would simplify the valve and allow for larger tolerances for proper performance. Magnetic cartridges would again be used to actuate the valve in a stemless design.

A MagBall concept replaces the rotating gate with a rotating ball. The ball does not rotate lock-step with the magnetic cartridge as the rotating gate did. Instead, the torque has a more complex rotation that allows the ball to go from fully open to fully closed.

Valves based on this concept are similar to standard ball valves, but they do not require an actuation stem as do other standard ball valves. Instead, this valve rotates the ball around a fixed axis by means of two guide pins. The two pins are guided by concentric grooves that interlock with the inner magnetic cartridge of the valve. This design is suited for magnetic actuation, and provides a leak-proof valve that can be used for hazardous gases and fluids.

The distinct advantages that this new design provides over previous VOST designs are the following:

- The passageway through the valve no longer has to be off-set as required by the rotating gate design. Instead, it can be machined through the center of the valve, using conventional boring techniques, and avoiding costly wire EDM (electrical discharge machining).
- The cross-sectional area of the passage through the ball is nearly twice the area provided by the hole in the rotating gate. Resistance to the fluid flow has been reduced by 40%. This is equivalent to gaining the advantage of the next pipe size larger without increasing the exterior size of the valve.
- The off-set venturi is no longer required for the best performance of the valve. This means that the previous minimum length requirements of the venturi are no longer neces-



The rotating venturi ramp of the original VOST design is replaced in the **Stainless Ball Valve** by a rotating, non-venturi gate.

sary. The valve can be shortened to meet ASME flange-to-flange dimensions in the 4-in. (≈ 10 -cm) and larger sizes without increasing the resistance to flow.

- Rotational requirements have been reduced from 180° to 90° . The valve can be actuated by standard quarter-turn actuators (without step-up gearing). This is the same type of actuation used with all ball, plug, and butterfly valves.

This work was done by Robert K. Burgess of Big Horn Valve, and David Yakos and Bryan Walthall of Salient Technologies for Johnson Space Center. For further information, contact

the JSC Innovation Partnerships Office at (281) 483-3809.

In accordance with Public Law 96-517, the contractor has elected to retain title to this invention. Inquiries concerning rights for its commercial use should be addressed to:

Robert K. Burgess, CEO

Big Horn Valve, Inc.

1664 Terra Ave., #5

Sheridan, WY 82801

Phone No.: (307) 672-0968

E-mail: kevin@bighornvalve.com

Refer to MSC-24602-1, volume and number of this NASA Tech Briefs issue, and the page number.



Improving Balance Function Using Low Levels of Electrical Stimulation of the Balance Organs

A device based on this technology may be used as a miniature patch worn by people with disabilities to improve posture and locomotion, and to enhance adaptability or skill acquisition.

Lyndon B. Johnson Space Center, Houston, TX

Crewmembers returning from long-duration space flight face significant challenges due to the microgravity-induced inappropriate adaptations in balance/sensorimotor function. The Neuroscience Laboratory at JSC is developing a method based on stochastic resonance to enhance the brain's ability to detect signals from the balance organs of the inner ear and use them for rapid improvement in balance skill, especially when combined with balance training exercises. This method involves a stimulus delivery system that is wearable/portable and provides imperceptible electrical stimulation to the balance organs of the human body.

Stochastic resonance (SR) is a phenomenon whereby the response of a nonlinear system to a weak periodic input signal is optimized by the presence of a particular non-zero level of noise. This phenomenon of SR is based on the concept of maximizing the flow of information through a system by a non-zero level of noise. Application of imperceptible SR noise coupled with sensory input in humans has been

shown to improve motor, cardiovascular, visual, hearing, and balance functions. SR increases contrast sensitivity and luminance detection; lowers the absolute threshold for tone detection in normal hearing individuals; improves homeostatic function in the human blood pressure regulatory system; improves noise-enhanced muscle spindle function; and improves detection of weak tactile stimuli using mechanical or electrical stimulation. SR noise has been shown to improve postural control when applied as mechanical noise to the soles of the feet, or when applied as electrical noise at the knee and to the back muscles.

SR using imperceptible stochastic electrical stimulation of the vestibular system (stochastic vestibular stimulation, SVS) applied to normal subjects has shown to improve the degree of association between the weak input periodic signals introduced via venous blood pressure receptors and the heart-rate responses. Also, application of SVS over 24 hours improves the long-term heart-rate dynamics and motor responsiveness as

indicated by daytime trunk activity measurements in patients with multi-system atrophy, Parkinson's disease, or both, including patients who were unresponsive to standard therapy for Parkinson's disease. Recent studies conducted at the NASA JSC Neurosciences Laboratories showed that imperceptible SVS, when applied to normal young healthy subjects, leads to significantly improved balance performance during postural disturbances on unstable compliant surfaces. These studies have shown the benefit of SR noise characteristic optimization with imperceptible SVS in the frequency range of 0–30 Hz, and amplitudes of stimulation have ranged from 100 to 400 microamperes.

This work was done by Jacob Bloomberg and Millard Reschke of Johnson Space Center; Ajitkumar Mulavara and Scott Wood of USRA; Jorge Serrador of Dept. of Veterans Affairs NJ Healthcare System; Matthew Fiedler, Igor Kofman, and Brian T. Peters of Wyle; and Helen Cohen of Baylor College. For further information, contact the JSC Innovation Partnerships Office at (281) 483-3809. MSC-25013-1



Oxygen-Methane Thruster

Marshall Space Flight Center, Alabama

An oxygen-methane thruster was conceived with integrated igniter/injector capable of nominal operation on either gaseous or liquid propellants. The thruster was designed to develop 100 lbf (≈ 445 N) thrust at vacuum conditions and use oxygen and methane as propellants. This continued development included refining the design of the thruster to minimize part count and manufacturing difficulties/cost, refining the modeling tools and capabilities that support system

design and analysis, demonstrating the performance of the igniter and full thruster assembly with both gaseous and liquid propellants, and acquiring data from this testing in order to verify the design and operational parameters of the thruster.

Thruster testing was conducted with gaseous propellants used for the igniter and thruster. The thruster was demonstrated to work with all types of propellant conditions, and provided the desired performance. Both the thruster

and igniter were tested, as well as gaseous propellants, and found to provide the desired performance using the various propellant conditions. The engine also served as an injector testbed for MSFC-designed refractory combustion chambers made of rhenium.

This work was done by Tim Pickens of Orion Propulsion, Inc. for Marshall Space Flight Center. For more information, contact Sammy Nabors, MSFC Commercialization Assistance Lead, at sammy.a.nabors@nasa.gov. Refer to MFS-32776-1.

Lunar Navigation Determination System — LaNDS

Goddard Space Flight Center, Greenbelt, Maryland

A portable comprehensive navigational system has been developed that both robotic and human explorers can use to determine their location, attitude, and heading anywhere on the lunar surface independent of external infrastructure (needs no Lunar satellite network, line of sight to the Sun or Earth, etc.). The system combines robust processing power with an extensive topographical database to create a real-time atlas (GIS — Geospatial Information System) that is able to autonomously control and monitor both single unmanned rovers and

fleets of rovers, as well as science payload stations. The system includes provisions for teleoperation and tele-presence. The system accepts (but does not require) inputs from a wide range of sensors.

A means was needed to establish a location when the search is taken deep in a crater (looking for water ice) and out of view of Earth or any other references. A star camera can be employed to determine the user's attitude in menial space and stellar map in body space. A local nadir reference (e.g., an accelerometer that orients the nadir

vector in body space) can be used in conjunction with a digital ephemeris and gravity model of the Moon to isolate the latitude, longitude, and azimuth of the user on the surface. That information can be used in conjunction with a Lunar GIS and advanced navigation planning algorithms to aid astronauts (or other assets) to navigate on the Lunar surface.

This work was done by David Quinn and Stephen Talabac of Goddard Space Flight Center. Further information is contained in a TSP (see page 1). GSC-15892-1

Launch Method for Kites in Low-Wind or No-Wind Conditions

Goddard Space Flight Center, Greenbelt, Maryland

Airborne observations using lightweight camera systems are desirable for a variety of applications. This system was contemplated as a method to provide a simple remote sensing aerial platform. Kites have been successfully employed for aerial observations, but have historically required natural wind or towing to become airborne. This new method negates this requirement, and widens the applicability of kites for carrying instrumentation. Applicability is primarily

limited by the space available on the ground for launching.

The innovation is a method for launching kites in low-wind or no-wind conditions. This method will enable instrumentation to be carried aloft using simple (or complex) kite-based systems, to obtain observations from an aerial perspective. This technique will provide access to altitudes of 100 meters or more over any area normally suited for kite flying. The duration of any observation is

dependent on wind strength; however, the initial altitude is relatively independent. The system does not require any electrical or combustion-based elements. This technology was developed to augment local-scale airborne measurement capabilities suitable for Earth science research, agricultural productivity, and environmental observations. The method represents an extension of techniques often used in aeronautical applications for launching fixed-wing

aircraft, such as sailplanes, using mechanical means not incorporated in the aircraft itself.

The innovation consists of an elastic cord (for propulsive force), a tether extension (optional, for additional height),

and the kite (instrumentation optional). Operation of the system is accomplished by fixing the elastic cord to ground (or equivalent), attaching the cord with/without a tether extension to the kite, tensioning the system to store energy,

and releasing the kite. The kite will climb until energy is dissipated.

This work was done by Geoffrey Bland and Ted Miles of Goddard Space Flight Center. Further information is contained in a TSP (see page 1). GSC-16004-1

Supercritical CO₂ Cleaning System for Planetary Protection and Contamination Control Applications

This system can be used for precision cleaning in optical and semiconductor applications.

NASA's Jet Propulsion Laboratory, Pasadena, California

Current spacecraft-compatible cleaning protocols involve a vapor degreaser, liquid sonication, and alcohol wiping. These methods are not very effective in removing live and dead microbes from spacecraft piece parts of slightly complicated geometry, such as tubing and loosely fitted nuts and bolts. Contamination control practices are traditionally focused on cleaning and monitoring of particulate and oily residual. Vapor degreaser and outgassing bake-out have not been proven to be effective in removing some less volatile, hydrophilic biomolecules of significant relevance to life detection.

A precision cleaning technology was developed using supercritical CO₂ (SCC). SCC is used as both solvent and carrier for removing organic and particulate contaminants. Supercritical fluid, like SCC, is characterized by physical and thermal properties that are between those of the pure liquid and gas phases. The fluid density is a function of the temperature and pressure. Its solvating power can be adjusted by changing the pressure or temperature, or adding a secondary solvent such as alcohol or water.

Unlike a regular organic solvent, SCC has higher diffusivities, lower viscosity, and lower surface tension. It readily penetrates porous and fibrous solids and can

reach hard-to-reach surfaces of the parts with complex geometry. Importantly, the CO₂ solvent does not leave any residue.

The results using this new cleaning device demonstrated that both supercritical CO₂ with 5% water as a co-solvent can achieve cleanliness levels of 0.01 mg/cm² or less for contaminants of a wide range of hydrophobicities. Experiments under the same conditions using compressed Martian air mix, which consists of 95% CO₂, produced similar cleaning effectiveness on the hydrophobic compounds.

The main components of the SCC cleaning system are a high-pressure cleaning vessel, a boil-off vessel located downstream from the cleaning vessel, a syringe-type high-pressure pump, a heat exchanger, and a back pressure regulator (BPR).

After soaking the parts to be cleaned in the clean vessel for a period, the CO₂ with contaminants is flushed out of the cleaning vessel using fresh CO₂ in a first-in-first-out (FIFO) method. The contaminants are either precipitating out in the boil-off container or being trapped in a filter subsystem. The parts to be cleaned are secured in a basket inside and can be rotated up to 1,400 rpm by a magnetic drive. The fluid flows within the vessel generate tangential forces on the parts' surfaces, enhancing

the cleaning effectiveness and shortening the soaking time.

During the FIFO flushing, the pump subsystem pushes fresh CO₂ into the cleaning vessel at a constant flow rate between 0.01 and 200 mL/min, while the BPR regulates the pressure in the cleaning vessel to within 0.1 bar by controlling the needle position in an outlet valve.

The fresh CO₂ gas flows through the heat exchanger at a given temperature before entering the cleaning vessel. A platinum resistance thermometer (PRT) reads the cleaning vessel interior temperature that can be controlled to within 0.1 K. As a result, cleaning vessel temperature remains constant during the FIFO flushing. There is no change in solvent power during FIFO flushing since both temperature and pressure inside the cleaning vessel remain unchanged, thus minimizing contaminants left behind. During decompression, both temperature and pressure are strictly controlled to prevent bubbles from generating in the cleaning vessel that could stir up the contaminants that sank to the bottom by gravity.

This work was done by Ying Lin, Fang Zhong, David C. Aveline, and Mark S. Anderson of Caltech for NASA's Jet Propulsion Laboratory. Further information is contained in a TSP (see page 1). NPO-47414

Design and Performance of a Wideband Radio Telescope

NASA's Jet Propulsion Laboratory, Pasadena, California

The Goldstone Apple Valley Radio Telescope (GAVRT) is an outreach project, a partnership involving NASA's Jet Propulsion Laboratory (JPL), the Lewis Center for Educational Research

(LCER), and the Apple Valley Unified School District near the NASA Goldstone deep space communication complex. This educational program currently uses a 34-meter antenna, DSS12,

at Goldstone for classroom radio astronomy observations via the Internet. The current program utilizes DSS12 in two narrow frequency bands around S-band (2.3 GHz) and X-band (8.45 GHz), and

is used by a training program involving a large number of secondary school teachers and their classrooms. To expand the program, a joint JPL/LCER project was started in mid-2006 to retrofit an additional existing 34-meter beam-waveguide antenna, DSS28, with wideband feeds and receivers to cover the 0.5-to-14-GHz frequency bands.

The DSS28 antenna has a 34-meter diameter main reflector, a 2.54-meter sub-reflector, and a set of beam waveguide mirrors surrounded by a 2.43-meter tube. The antenna was designed for

high power and a narrow frequency band around 7.2 GHz. The performance at the low end of the frequency band desired for the educational program would be extremely poor if the beam waveguide system was used as part of the feed system. Consequently, the 34-meter antenna was retrofitted with a tertiary offset mirror placed at the vertex of the main reflector. The tertiary mirror can be rotated to use two wideband feeds that cover the 0.5-to-14-GHz band.

The earlier designs for both GAVRT and the DSN only used narrow band

feeds and consequently, only covered a small part of the S- and X-band frequencies. By using both a wideband feed and wideband amplifiers, the entire band from 0.5 to 14 GHz is covered, expanding significantly the science activities that can be studied using this system.

This work was done by Sander Weinreb, William A. Imbriale, Glenn Jones, and Handi Mani of Caltech for NASA's Jet Propulsion Laboratory. For more information, contact iaoffice@jpl.nasa.gov. NPO-46668



▶ Finite Element Models for Electron Beam Freeform Fabrication Process

Potential applications are in the fabrication of short-run components, and repair and refurbishment of parts in the aerospace, automotive, power generation, and other industries.

Lyndon B. Johnson Space Center, Houston, Texas

Electron beam freeform fabrication (EBF³) is a member of an emerging class of direct manufacturing processes known as solid freeform fabrication (SFF); another member of the class is the laser deposition process. Successful application of the EBF³ process requires precise control of a number of process parameters such as the EB power, speed, and metal feed rate in order to ensure thermal management; good fusion between the substrate and the first layer and between successive layers; minimize part distortion and residual stresses; and control the microstructure of the finished product.

This is the only effort thus far that has addressed computer simulation of the EBF³ process. The models developed in this effort can assist in reducing the number of trials in the laboratory or on the shop floor while making high-quality parts. With some modifications, their use can be further extended to the simulation of laser, TIG (tungsten inert gas), and other deposition processes.

A solid mechanics-based finite element code, ABAQUS, was chosen as the primary engine in developing these models whereas a computational fluid dynamics (CFD) code, Fluent, was used in a support role. Several innovative concepts were developed, some of which are

highlighted below. These concepts were implemented in a number of new computer models either in the form of standalone programs or as user subroutines for ABAQUS and Fluent codes.

A database of thermo-physical, mechanical, fluid, and metallurgical properties of stainless steel 304 was developed. Computing models for Gaussian and raster modes of the electron beam heat input were developed. Also, new schemes were devised to account for the heat sink effect during the deposition process. These innovations, and others, lead to improved models for thermal management and prediction of transient/residual stresses and distortions.

Two approaches for the prediction of microstructure were pursued. The first was an empirical approach involving the computation of thermal gradient, solidification rate, and velocity (G, R, V) coupled with the use of a solidification map that should be known *a priori*. The second approach relies completely on computer simulation. For this purpose a criterion for the prediction of morphology was proposed, which was combined with three alternative models for the prediction of microstructure; one based on solidification kinetics, the second on phase diagram, and the third on differ-

ential scanning calorimetry data. The last was found to be the simplest and the most versatile; it can be used with multi-component alloys and rapid solidification without any additional difficulty.

For the purpose of (limited) experimental validation, finite element models developed in this effort were applied to three different shapes made of stainless steel 304 material, designed expressly for this effort with an increasing level of complexity.

These finite element models require large computation time, especially when applied to deposits with multiple adjacent beads and layers. This problem can be overcome, to some extent, by the use of fast, multi-core computers. Also, due to their numerical nature coupled with the fact that solid mechanics-based models are being used to represent the material behavior in liquid and vapor phases as well, the models have some inherent approximations that become more pronounced when dealing with multi-bead and multi-layer deposits.

This work was done by Umesh Chandra of Modern Computational Technologies, Inc. for Johnson Space Center. Further information is contained in a TSP (see page 1). MSC-24598-1

▶ Autonomous Information Unit for Fine-Grain Data Access Control and Information Protection in a Net-Centric System

Potential uses include cyber-security, smart grid, defense networks, and enterprise networks.

NASA's Jet Propulsion Laboratory, Pasadena, California

As communication and networking technologies advance, networks will become highly complex and heterogeneous, interconnecting different network domains. There is a need to provide user authentication and data protection in order to further facilitate

critical mission operations, especially in the tactical and mission-critical net-centric networking environment. The Autonomous Information Unit (AIU) technology was designed to provide the fine-grain data access and user control in a net-centric system-testing environ-

ment to meet these objectives.

The AIU is a fundamental capability designed to enable fine-grain data access and user control in the cross-domain networking environments, where an AIU is composed of the mission data, metadata, and policy. An AIU pro-

vides a mechanism to establish trust among deployed AIUs based on recombining shared secrets, authentication and verify users with a username, X.509 certificate, enclave information, and classification level. AIU achieves data protection through (1) splitting data into multiple information pieces using the Shamir's secret sharing algorithm, (2) encrypting each individual information piece using military-grade AES-256 encryption, and (3) randomizing the position of the encrypted data based on the unbiased and memory efficient in-place Fisher-Yates shuffle method. Therefore, it becomes virtually impossi-

ble for attackers to compromise data since attackers need to obtain all distributed information as well as the encryption key and the random seeds to properly arrange the data. In addition, since policy can be associated with data in the AIU, different user access and data control strategies can be included.

The AIU technology can greatly enhance information assurance and security management in the bandwidth-limited and ad hoc net-centric environments. In addition, AIU technology can be applicable to general complex network domains and applications where distributed user authentication and data protection are

necessary. AIU achieves fine-grain data access and user control, reducing the security risk significantly, simplifying the complexity of various security operations, and providing the high information assurance across different network domains.

This work was done by Edward T. Chow, Simon S. Woo, Mark James, and George K. Palouljian of Caltech for NASA's Jet Propulsion Laboratory. Further information is contained in a TSP (see page 1).

This software is available for commercial licensing. Please contact Daniel Broderick of the California Institute of Technology at danielb@caltech.edu. Refer to NPO-48224.

➤ Vehicle Detection for RCTA/ANS (Autonomous Navigation System)

This algorithm can be applied to semi-autonomous vehicles for driver assistance, and to military robots.

NASA's Jet Propulsion Laboratory, Pasadena, California

Using a stereo camera pair, imagery is acquired and processed through the "JPLV" stereo processing pipeline. From this stereo data, large 3D blobs are found. These blobs are then described and classified by their shape to determine which are vehicles and which are not. Prior vehicle detection algorithms are either targeted to specific domains, such as following lead cars, or are intensity-based methods that involve learning typical vehicle appearances from a large corpus of training data.

In order to detect vehicles, the JPL Vehicle Detection (JVD) algorithm goes through the following steps:

1. Take as input a left disparity image and left rectified image from JPLV stereo.

2. Project the disparity data onto a two-dimensional Cartesian map.

3. Perform some post-processing of the map built in the previous step in order to clean it up.

4. Take the processed map and find peaks. For each peak, grow it out into a map blob. These map blobs represent large, roughly vehicle-sized objects in the scene.

5. Take these map blobs and reject those that do not meet certain criteria. Build descriptors for the ones that remain. Pass these descriptors onto a classifier, which determines if the blob is a vehicle or not.

The probability of detection is the probability that if a vehicle is present in the image, is visible, and un-occluded,

then it will be detected by the JVD algorithm. In order to estimate this probability, eight sequences were ground-truthed from the RCTA (Robotics Collaborative Technology Alliances) program, totaling over 4,000 frames with 15 unique vehicles. Since these vehicles were observed at varying ranges, one is able to find the probability of detection as a function of range. At the time of this reporting, the JVD algorithm was tuned to perform best at cars seen from the front, rear, or either side, and perform poorly on vehicles seen from oblique angles.

This work was done by Shane Brennan, Max Bajracharya, Larry H. Matthies, and Andrew B. Howard of Caltech for NASA's Jet Propulsion Laboratory. Further information is contained in a TSP (see page 1). NPO-47569

➤ Image Mapping and Visual Attention on the Sensory Ego-Sphere

This technology can be used to map a robot's environment and direct its attention.

Lyndon B. Johnson Space Center, Houston, Texas

The Sensory Ego-Sphere (SES) is a short-term memory for a robot in the form of an egocentric, tessellated, spherical, sensory-motor map of the robot's locale. Visual attention enables fast alignment of overlapping images without warping or position optimization, since an attentional point (AP) on the

composite typically corresponds to one on each of the collocated regions in the images. Such alignment speeds analysis of the multiple images of the area.

Compositing and attention were performed two ways and compared: (1) APs were computed directly on the composite and not on the full-resolution images until

the time of retrieval; and (2) the attentional operator was applied to all incoming imagery. It was found that although the second method was slower, it produced consistent and, thereby, more useful APs.

The SES is an integral part of a control system that will enable a robot to learn new behaviors based on its previ-

ous experiences, and that will enable it to recombine its known behaviors in such a way as to solve related, but novel, task problems with apparent creativity. The approach is to combine sensory-motor data association and dimensionality reduction to learn navigation and manipulation tasks as sequences of basic behaviors that can be implemented with a small set of closed-loop controllers. Over time, the aggregate of behaviors and their transition probabilities form a stochastic network. Then given a task, the robot finds a path in the network that leads from its current

state to the goal.

The SES provides a short-term memory for the cognitive functions of the robot, association of sensory and motor data via spatio-temporal coincidence, direction of the attention of the robot, navigation through spatial localization with respect to known or discovered landmarks, and structured data sharing between the robot and human team members, the individuals in multi-robot teams, or with a C3 center.

This work was done by Katherine Achim Fleming and Richard Alan Peters II of Vanderbilt University for Johnson Space Center.

Further information is contained in a TSP (see page 1).

In accordance with Public Law 96-517, the contractor has elected to retain title to this invention. Inquiries concerning rights for its commercial use should be addressed to:

*Vanderbilt University, School of Engineering
Department of Electrical Engineering and
Computer Science*

*VU Station B 351824,
2301 Vanderbilt Place
Nashville, TN 37235*

Refer to MSC-24363-1, volume and number of this NASA Tech Briefs issue, and the page number.

▶ HyDE Framework for Stochastic and Hybrid Model-Based Diagnosis

It uses hybrid models built by the users and sensor data from the system to deduce the state of the system over time.

Ames Research Center, Moffett Field, California

Hybrid Diagnosis Engine (HyDE) is a general framework for stochastic and hybrid model-based diagnosis that offers flexibility to the diagnosis application designer. The HyDE architecture supports the use of multiple modeling paradigms at the component and system level. Several alternative algorithms are available for the various steps in diagnostic reasoning. This approach is extensible, with support for the addition of new modeling paradigms as well as diagnostic reasoning algorithms for existing or new modeling paradigms.

HyDE is a general framework for stochastic hybrid model-based diagnosis of discrete faults; that is, spontaneous changes in operating modes of components. HyDE combines ideas from consistency-based and stochastic approaches to model-based diagnosis using discrete and continuous models to create a flexible and extensible architecture for stochastic and hybrid diagnosis. HyDE supports the use of multiple paradigms and

is extensible to support new paradigms.

HyDE generates candidate diagnoses and checks them for consistency with the observations. It uses hybrid models built by the users and sensor data from the system to deduce the state of the system over time, including changes in state indicative of faults.

At each time step when observations are available, HyDE checks each existing candidate for continued consistency with the new observations. If the candidate is consistent, it continues to remain in the candidate set. If it is not consistent, then the information about the inconsistency is used to generate successor candidates while discarding the candidate that was inconsistent.

The models used by HyDE are similar to simulation models. They describe the expected behavior of the system under nominal and fault conditions. The model can be constructed in modular and hierarchical fashion by building component/subsystem models (which

may themselves contain component/subsystem models) and linking them through shared variables/parameters. The component model is expressed as operating modes of the component and conditions for transitions between these various modes. Faults are modeled as transitions whose conditions for transitions are unknown (and have to be inferred through the reasoning process).

Finally, the behavior of the components is expressed as a set of variables/parameters and relations governing the interaction between the variables. The hybrid nature of the systems being modeled is captured by a combination of the above transitional model and behavioral model. Stochasticity is captured as probabilities associated with transitions (indicating the likelihood of that transition being taken), as well as noise on the sensed variables.

This work was done by Sriram Narasimhan and Lee Brownston of Ames Research Center. Further information is contained in a TSP (see page 1). ARC-15570-1

▶ IMAGESEER — IMAGEs for Education and Research

Web portal shares image data with research institutions.

Goddard Space Flight Center, Greenbelt, Maryland

IMAGESEER is a new Web portal that brings easy access to NASA image data for non-NASA researchers, educators,

and students. The IMAGESEER Web site and database are specifically designed to be utilized by the university community,

to enable teaching image processing (IP) techniques on NASA data, as well as to provide reference benchmark data to

validate new IP algorithms. Along with the data and a Web user interface front-end, basic knowledge of the application domains, benchmark information, and specific NASA IP challenges (or case studies) are provided.

Working with project scientists and engineers, four types of IP techniques have been identified as corresponding to Earth Science needs; these are gap filling/in-painting, cloud detection, image registration, and map cover/classification. For each of these challenges, corresponding data were selected from four different geographic regions: mountains (Colorado), urban (Los Angeles), water coastal area (Chesapeake Bay), and agriculture (Illinois). Satellite images have been collected for these areas from several satellite instruments, then georegistered, and finally converted to common image formats (GeoTIFF and raw). Along with the original data, associated benchmarks (or validation data) have been acquired or generated, including cloud cover masks and assessments, georegistered scenes, and

classification maps from the National Land Cover Data (NLCD) database gathered in 1992 and 2001 by the Multi-Resolution Land Characteristics Consortium (MRLC).

IMAGESEER provides a modern and graphically-rich Web site (<http://imageseer.nasa.gov>) for easily browsing and downloading all of the selected datasets, benchmarks, and tutorials. Using a paradigm common on commercial Web sites, users can restrict their searches by selectively filtering by data source (project, mission, and instrument), region of interest, desired image processing technique, and time period. By deliberately focusing on only a subset of NASA data, continuously emphasizing ease-of-use, providing common file formats, and supplying the “answers” as well as the questions to NASA IP challenges, IMAGESEER provides an easily navigable and usable Web site for non-NASA researchers, educators, and students. On the backend, automated Python scripts convert the NASA data, generate thumbnails and

benchmarks, and populate the IMAGESEER database. The database and the IMAGESEER Web site were developed using a MySQL database and HyperText PreProcessor (PHP).

IMAGESEER currently focuses on Earth Science data, but is designed to be straightforwardly extended to planetary and exploration data, and in fact, planetary-specific challenges, such as automated crater counting and boulder counting, have already been identified. IMAGESEER is ideal for helping educators and students learn IP techniques needed for and with actual NASA data and for helping researchers develop new algorithms or adapt existing algorithms to NASA data and challenges. It provides a focused set of NASA-centric data for education and research, hopefully engendering further interest in NASA careers and research.

This work was performed by Jacqueline Le Moigne, Thomas Grubb, and Barbara Milner for Goddard Space Flight Center. Further information is contained in a TSP (see page 1). GSC-15967-1



National Aeronautics and
Space Administration